Published in final edited form as:
J Neurosci Methods. 2011 March 15; 196(1): 51–59. doi:10.1016/j.jneumeth.2010.12.025.

Amyloid-β42 Alters Apolipoprotein E Solubility in Brains of Mice with Five Familial AD Mutations

Katherine Lynn Youmans[1], **Steffi Leung**[1], **Juan Zhang**[3], **Erika Maus**[2], **Kathleen Baysac**[3], **Guojun Bu**[3,†], **Robert Vassar**[2], **Chunjiang Yu**[1], and **Mary Jo LaDu**[1,*]

[1]Dept of Anatomy and Cell Biology, University of Illinois at Chicago, Chicago, IL 60612

[2]Dept of Cell and Molecular Biology, Northwestern University, Chicago, IL 60611

[3]Dept of Pediatrics, Cell Biology and Physiology, Washington University School of Medicine, St. Louis, MO 63110

Abstract

Amyloid plaques composed of the 42 amino acid form of amyloid-beta peptide (Aβ42) are a pathological hallmark of Alzheimer's disease (AD), but soluble and intraneuronal Aβ42 are the more proximal causes of synaptic dysfunction and neurotoxicity. Apolipoprotein E (apoE) modulates this disease process, as inheritance of the ε4 allele of the apoE gene is the primary genetic *risk* factor for AD. To address the solubility of Aβ42 and apoE, a protein extraction protocol in the presence of minimal to extensive Aβ42 pathology was optimized. Sequential extractions with TBS, TBS+Triton X-100 (TBSX), and guanidine-HCl (GuHCl) or formic acid (FA) were used with tissue from young and old wild type or mice expressing 5 familial AD mutations (5xFAD), in disease-susceptible or –resistant brain regions. In older 5xFAD mice, the extraction of insoluble Aβ42 and m-apoE protein was increased with FA compared to GuHCl. The 5 FAD mutations significantly increase production of Aβ42, recapitulating AD-like pathology at a greatly accelerated rate. Consistent protein extraction and the specificity of extractions for soluble or membrane-associated proteins were demonstrated. Age-dependent increases in Aβ42 were observed in all extraction fractions, particularly in the cortex and hippocampus. In both young and old 5xFAD mice, Aβ42 is TBS- or GuHCl-soluble. While in WT mice m-apoE is TBSX-soluble, in 5xFAD mice m-apoE is TBS- or GuHCl-soluble. Thus, the extraction profile of Aβ42 paralleled that of m-apoE in 5xFAD mice. As now characterized, this method identifies the extraction profile for disease-relevant brain proteins, both normal or modified due to neuropathological processes.

Complete Addresses and Contact Information for All Authors: Katherine L. Youmans, Steffi Leung, Chunjiang Yu and Mary Jo LaDu, Department of Anatomy, UIC, 808 S. Wood St., CME Room 578, MC 512, Chicago, IL 60612, kyouma2@uic.edu, cjyu@uic.edu, sleung7@uic.edu, mladu@uic.edu, Phone: (312) 355-2994, Fax: (312) 355-0386; Juan Zhang, Kathleen Baysac, Dept of Pediatrics, Washington University School of Medicine, Bu lab, 4938 Parkview Place, St. Louis, MO 63110, Zhang_J@kids.wustl.edu, kcbaysac@gmail.com, Phone: (314) 286-2860, Fax: (314) 286-2894; Guojun Bu, Department of Neuroscience, Mayo Clinic, 4500 San Pablo Road, Jacksonville, FL 32224, bu.guonjun@mayo.edu, phone: (904) 953-0158; Erika Maus, Robert Vassar, Dept of Cell and Molecular Biology, Northwestern University, 303 E. Chicago Ave., Tarry 8-720, Chicago, IL 60611, e-maus@northwestern.edu, r-vassar@northwestern.edu, Phone: (312) 503-3361, Fax: (312) 503-7912. *Corresponding author information: Mary Jo LaDu, Department of Anatomy, UIC, 808 S. Wood St., CME Rm 578, MC 512, Chicago, IL 60612, mladu@uic.edu, Phone: (312) 355-4795, Fax: (312) 355-0386.
†Present affiliation: Department of Neuroscience, Mayo Clinic, Jacksonville, FL 32224

Keywords

Alzheimer's disease; apoE; detergent; 5xFAD; solubility

1. Introduction[1]

Alzheimer's disease (AD), the most common form of dementia in the aged, is defined by memory deficits and cognitive decline that result from brain region-specific neuronal loss (Querfurth and LaFerla, 2010). Extracellular amyloid plaques composed primarily of the 42 amino acid isoform of amyloid-β peptide (Aβ42) are a pathological hallmark of AD. However, soluble and intraneuronal Aβ appear prior to plaque deposition and are more closely associated with the earliest markers of synaptic loss and neurotoxicity (Aoki et al., 2008; Christensen et al., 2010; Thal et al., 2006; Tomiyama et al., 2010; Yu et al., 2010a). However, identifying and isolating this non-plaque form of Aβ42 has proven to be difficult. In addition, inheritance of the ε4 allele of the apolipoprotein E (apoE) gene increases the risk for AD 4- to 8-fold compared to ε3, the most common allele, and ε2 reduces AD risk 2- to 4-fold. ApoE is the primary genetic risk factor for sporadic AD; it influences Aβ deposition (Caselli et al., 2010) and potentially modulates the formation and function of soluble and intracellular Aβ (Kim et al., 2009). Currently, research focuses on identifying the sequence of molecular events that occur during the development of Aβ pathology, particularly the changing interactions between Aβ42 and apoE.

Various *in vitro* and *in vivo* analyses have attributed Aβ-induced neurotoxicity to soluble pools of Aβ42 (Cizas et al., 2010; Durakoglugil et al., 2009; Ohno et al., 2006). While immunohistochemical (IHC) techniques or plaque-specific stains can detect regional

[1]Abbreviations:

Aβ	amyloid-β
apoE	apolipoprotein E
TBS	tris-buffered saline
TBSX	TBS + Triton X-100
GuHCl	guanidine-HCl
FA	formic acid
m-apoE	murine apoE
5xFAD	5 familial AD mutations
Aβ-Tg	mice overproducing Aβ
IHC	immunohistochemistry
APP	amyloid precursor protein
WT	wild type
CX	cortex
H	hippocampus
CB	cerebellum
SnT	supernatant
LAMP1	lysosome-associated membrane protein 1

accumulation of intraneuronal Aβ and deposition of extracellular amyloid (Belinson et al., 2008; Cataldo et al., 2004; Oakley et al., 2006; Oddo et al., 2003; Schmitz et al., 2004), these methods are not well-suited for identifying the solubility of the peptide. In addition, the labile nature of Aβ42 assemblies *in vitro* and *in vivo* limits the accuracy of most biochemical extraction/isolation/purification methods. Further, Aβ pathology is very brain region-specific in both humans and mice, making it necessary to distinguish between disease-susceptible vs disease-resistant regions. This is particularly important for determining whether memory loss is hippocampal-dependent vs -independent (Ohno et al., 2006). For these reasons, one goal of the current experiments was to develop a sequential protein extraction method for quantifying soluble and insoluble Aβ in defined brain regions, rather than whole-brain homogenates.

Current research has focused on soluble forms of apoE in the brain, largely because of the toxicity associated with soluble Aβ42 (Bales et al., 2009; Sullivan et al., 2009). However, apoE contains a c-terminal lipid-binding domain and is predominantly localized to lipoprotein particles or vesicles, requiring the presence of detergents for extraction from tissue (Han et al., 1994; Krul and Cole, 1996; Lippel et al., 1983; Yu et al., 2010b). Further, analyzing tissue that has been extracted with only TBS followed by GuHCl can be problematic due to apoE preferentially segregating to the lipid phase during extraction (Sullivan et al., 2009). Extraction methods have previously been optimized for specific proteins, although comparing results between protocols can be difficult because of the varying homogenization methods, number of extraction steps, extraction buffers, type and concentration of detergents, and centrifugation methods, as well as the source of tissue, whether whole-brains or dissected regions, or from mouse or human samples (Brecht et al., 2004; Elliott et al., 2009; Hirsch-Reinshagen et al., 2005; Kawarabayashi et al., 2004; Kawarabayashi et al., 2001; Lesne et al., 2006; Oakley et al., 2006; Sullivan et al., 2009; Zerbinatti et al., 2006; Zhao et al., 2007). For example, efforts have been made to identify the specific cellular localization of Aβ based on its extraction fraction (Gouras et al., 2010). Thus, a combination of these previously described extraction protocols designed to specifically evaluate the solubility and levels of Aβ42 and apoE will provide further information on the interactions between these two AD-relevant proteins.

Aβ42 likely drives AD-associated Aβ pathology. However, many previously generated mice expressing mutations in genes that increase the production of Aβ (Aβ-Tg mice; for example, (Mastrangelo and Bowers, 2008)) produce predominantly Aβ40. In addition, the onset of pathology may not begin until >10 months of age in these mice, making the design of experimental interventions long and tedious. The mutations in mice expressing 5 FAD mutations (5xFAD mice) act additively to increase Aβ42 production, largely due to elevated β-site APP cleaving enzyme-1 (BACE1) (Zhao et al., 2007), resulting in intraneuronal Aβ by 6 weeks followed immediately by plaques at 2 months (Oakley et al., 2006). While biochemical analyses confirmed significantly elevated Aβ42 levels with age in whole-brain homogenates from 5xFAD mice (Ohno et al., 2006), the region-specific extraction profile for Aβ42, as well as the extraction profile for apoE in the absence or presence of Aβ42 pathology, remains unknown. For the present study, a working protocol was established for the serial extraction of proteins specifically into the TBS-, detergent-, and guanidine HCl-(GuHCl) or formic acid (FA)-soluble fractions of the cortex, hippocampus and cerebellum of young and old mice. This extraction protocol was used to determine the solubility and levels of Aβ42 and their effects on m-apoE. In 5xFAD mice, Aβ42 extracts primarily in the TBS and GuHCl fractions of disease-susceptible brain regions, with levels increasing significantly with age. Of particular interest, m-apoE in WT mice extracted predictably in the TBSX fraction, but in the presence of increasing amounts of Aβ42 the extraction shifted to the TBS and GuHCl fractions, though total m-apoE levels were relatively unchanged

from 2 to 6 months. The extraction profile for m-apoE in 5xFAD mice mirrored that for Aβ42. Thus, an opportunity for apoE:Aβ42 interactions was identified.

2. Materials and Methods

2.1 Animals and brain dissection

All experiments follow the UIC Institutional Animal Care and Use Committee protocols. Mice are housed under standard conditions with access to food and water *ad libitum*. 2- and 6-month-old inbred c57Bl/6 mice as WT were purchased from Jackson, 2- and 6-month-old outbred 5xFAD mice were obtained from Robert Vassar (Northwestern (Oakley et al., 2006)), and 9-month-old 5xFAD mice were from a colony maintained by the LaDu lab (Taconic labs). 5xFAD mice express 5 familial AD mutations (3xAPP [K670N/M671L (Swedish) + I716V ([Florida) + V717I (London) and 2xPS1 [M146L+L286V]), with neuronal expression driven by the Thy-1 promoter. The brains of all mice were removed and dissected at the midline as described (Oakley et al., 2006). The right hemibrains from mice at each age were rapidly dissected on ice into cortex (CX), hippocampus (H) and cerebellum (CB). Brain regions were weighed on an analytical balance, immediately snap frozen in liquid nitrogen, and stored at −80°C until use. Wet weights of tissue were used for homogenization volumes (as weight/volume [w/v]), as described in detail below.

2.2 Reagents

Source of Antibodies: For Western blots, antibodies raised against the following proteins were used: lysosome-associated membrane protein 1 (LAMP1) (rat; 1:500; Santa Cruz), Akt1/2/3 (rabbit; 1:1000; Santa Cruz), αtubulin (rabbit, clone DM1A; 1:10,000; Abcam), APP (rabbit; 22C11; 1:2000; Millipore), m-apoE (rabbit; 1:2000; Biodesign). HRP-conjugated secondary antibodies raised against the following species were used at 1:5000 dilutions: rat (goat; Santa Cruz), mouse (rabbit; Jackson), and rabbit (goat; Jackson).

Homogenization/extraction buffer compositions: For protein extractions, brain tissue was homogenized in Tris-buffered saline (TBS) containing 1xProtease Inhibitor cocktail set 3 (PIC; Calbiochem) + 1xPhosphatase Inhibitor Cocktail sets 1+2 (PhIC) (Calbiochem). All subsequent extraction buffers also contained 1xPIC + 1xPhIC, as listed below.

2.3 Protein Extraction

Frozen tissue from dissected brains was placed into 1-3ml ice-cold glass dounce homogenizers containing 15 volumes (w/v) of Tris-buffered saline (TBS) homogenization buffer. Samples on ice were homogenized in a cold room (4°C) with 30 strokes in the glass dounces, transferred to pre-chilled 1.5ml polyallomer ultracentrifuge tubes (Fisher 357488) and centrifuged at 100,000xg for 1hr at 4°C using a TLA-55 rotor in an Optima TLX Ultracentrifuge (Beckman Coulter). The first supernatant (SnT-1), *TBS-soluble fraction*, was aliquoted into separate 0.6 ml tubes prior to freezing in liquid nitrogen and storage at −80°C. The pellet was washed with 200μl TBS buffer, centrifuged at 14,000xg for 5min at 4°C, and the wash discarded to prevent dilution of samples or potential contamination from disturbed pellet material. Pellets were resuspended in 15 volumes (w/v of tissue) of TBS buffer containing 1% Triton X-100 (TBSX) and mixed gently by rotation at 4°C for 30min, followed by a second centrifugation at 100,000xg for 1hr at 4°C. This SnT-2, *TBSX-soluble fraction*, was aliquoted and frozen as for TBS. The pellet was washed with TBSX buffer that was discarded. The TBSX-insoluble pellet was resuspended into 400μl of 5M GuHCl, mixed by rotation at room temperature for 6hrs, and centrifuged at 16,000xg for 30min. This SnT-3, *GuHCl-soluble fraction*, was aliquoted and frozen as described. See Figure 1 for a simplified overview of serial extraction steps.

To determine the extraction efficiency for Aβ42 and m-apoE, GuHCl was compared to 70% FA in parallel extractions of 9-month-old 5xFAD mice, where Aβ burden is extensive. The CX and CB were extracted as before with the following modifications: Following the rotation of samples in TBSX for 30min, each sample was divided equally into 2×1.5ml tubes for ultracentrifugation and the TBSX-insoluble pellets were then resuspended into either: 1) 200μl of GuHCl for 6hrs, or 2) 70% FA to bring samples to 150mg/ml for 2hrs. GuHCl-samples were centrifuged at 16,000xg for 30min at 4°C and this SnT is the *GuHCl-soluble fraction*. FA-samples were centrifuged at 100,000xg for 1hr at 4°C and this SnT is the *FA-soluble fraction*. FA-soluble fractions were neutralized by the addition of 20 volumes 1M Tris base, aliquoted and frozen at −80°C. See Figure 6A for a brief overview of these modifications to serial extraction steps.

Total protein content in TBS-, TBSX- and GuHCl-extractions was determined via colorimetric micro-BCA assay per manufacturer's instructions (Pierce #23225). Due to interference of Tris and FA with the BCA assay, total protein in FA-extractions was determined via Quick Start Bradford Protein micro-Assay, per manufacturer's instructions (Bio-Rad #500-0205).

2.4 Western Blot Analyses

25μg of total protein was incubated with loading buffer (5% β-mercaptoethanol + 1xLDS sample buffer [Invitrogen]), incubated for 10min at 70°C, and loaded into wells of 4-12% Bis-Tris NuPAGE precast gels (Invitrogen). Following electrophoresis, proteins were transferred onto 0.2μm PVDF membranes (Invitrogen), incubated in 5% (w/v) nonfat dry milk in TBS + Tween-20 + 1mM NaF (a phosphatase inhibitor) for 1hr, and with primary antibodies at 4°C for 2hr-overnight. Membranes were then washed in blocking solution, incubated with HRP-conjugated secondary antibodies for 45min, washed again, developed with Pierce chemiluminescence reagents, and visualized with a Kodak Image Station 4000R.

2.5 ELISA Analyses

Aβ42: To determine Aβ42 levels in extractions from 2-, 6- and 9-month-old 5xFAD mice, human Aβ42 ELISA kits of the same lot (Wako #298-62401) were used according to manufacturer's specifications. Briefly, samples were diluted in sample diluent to bring Aβ42 levels within an optimized working range of Aβ42 standards at known concentrations (0-100 pM) for each extraction buffer condition: 2-month mice: TBS- and TBSX-extractions = 1:5, GuHCl-extractions = 1:1000; 6-month mice: TBS-extractions = 1:25, TBSX-extractions = 1:10, GuHCl-extractions = 1:25,000; 9-month mice: GuHCl-extractions = 1:25,000, FA-extractions = 1:25,000 (after neutralization with 1M Tris, as described previously). All Aβ42 standards contained TX-100, GuHCl or FA at concentrations equivalent to those in the assayed samples, respectively. Following incubation with antibody solutions, the Aβ42 concentration in the samples was determined by colorimetric assay. The colorimetric reaction was terminated by the addition of stop solution (supplied) and the absorbance at 450nm (A_{450}) was recorded. A_{450} values were converted to pg Aβ42/mg tissue by comparing samples to the Aβ42 standard curves in the corresponding buffer conditions, correcting for respective dilution factors, and dividing by the weight of tissue.

Murine apoE: To determine levels of m-apoE in extractions from WT and 5xFAD mice, samples were diluted to bring m-apoE levels within an optimized working range of m-apoE standards at known concentrations (0-100 ng/well) for each extraction buffer condition: 2- and 6-month WT mice: TBS = 1:15, TBSX = 1:5, GuHCl = 1:10. For 2- and 6-month 5xFAD mice: TBS- and TBSX-extractions = 1:20, GuHCl-extractions =1:10; 9-month WT and 5xFAD mice: GuHCl-extractions = 1:20, FA-extractions = 1:5. All apoE standards contained TX-100, GuHCl or FA at concentrations equivalent to those in the assayed

samples, respectively. Samples were analyzed as described previously (Liu et al., 2007; Wahrle et al., 2007). Briefly, samples were incubated in a capture antibody WUE4 (David Holtzman, Washington University, St. Louis). M-apoE was detected by a primary antibody (anti-m-apoE; Calbiochem) and HRP-conjugated secondary antibody (anti-goat-HRP). The absorbance at 650nm (A_{650}) was recorded, and values were converted to ng apoE/mg tissue by comparing samples to the m-apoE standard curves in the corresponding buffer conditions, correcting for respective dilution factors, and dividing by the weight of tissue.

2.6 Statistics

Quantifications of Western blot membranes for αtubulin, APP and synaptic proteins were performed using ImageJ software, comparing band intensities of samples run within the same gel. For APP, αtubulin was used as a loading control and values are expressed as the change from age-matched WT controls (2 or 6 months). Statistical significance was established in Excel by two-tailed Student's t-Test analysis for p-values < 0.05 or 0.01 (as indicated in figure legends), for comparison between groups. n = 5 for 5xFAD mice at each age.

For Aβ42 and m-apoE measurements by ELISA, statistical significance for 2- and 6-month-old mice was established in Excel by two-tailed Student's t-Test analysis for p-values < 0.05, 0.01 or 0.001 (as indicated in figure legends), for comparison between groups. For parallel extractions of the same sample from 9-month-old mice (in GuHCl or FA; Figure 6), statistical significance was established in Excel by paired Student's t-Test analysis (David and Gunnink, 1997) for p-values < 0.05 or 0.001. n = 5 for 5xFAD mice at 9 months.

3. Results

3.1 Extraction Method

To optimize sequential protein extraction in the presence of increasing amounts of Aβ42 in the brain, 5xFAD mice aged 2, 6 or 9 months were compared to WT mice of the same ages. Extractions were initially based on previously published (Hirsch-Reinshagen et al., 2005; Kawarabayashi et al., 2001; Lesne et al., 2006) and unpublished protocols (LaDu and Bu labs', unpublished observations). First, to establish the reproducibility of homogenizations of small tissue-volumes by glass dounce, α-tubulin levels from TBS extractions were determined for the cortex, hippocampus and cerebellum of 2- and 6-month-old 5xFAD mice. Results demonstrate that α-tubulin protein levels within each brain region of 5xFAD mice at 2 and 6 months were consistently extracted. Representative Western blots and quantitative analyses from TBS-extracted α-tubulin are shown in Figure 2A.

Next, the extraction specificity for soluble and membrane-associated proteins was determined using proteins known to be enriched in specific fractions. The TBS, TBSX, and GuHCl fractions were analyzed by Western blot for Akt protein (a cytosolic protein used as a marker for TBS-soluble extractions) and LAMP1 (an integral membrane protein used as a marker for TBSX-soluble extractions). As shown in Figure 2B, Akt is enriched in the TBS-extractions and LAMP1 is localized to the TBSX-extractions in both 2-month WT and 9-month 5XFAD mice, with neither protein detected in the GuHCl fraction. In addition, APP was used as an AD relevant protein with a TBS-soluble (sAPP) and TBSX-soluble (full-length; flAPP) form. Antibodies specific for the N-terminus of APP detected C-terminal truncated sAPP migrating at approximately 85kDa in the TBS fractions of the cortex and hippocampus (Figures 2C and 3A). Membrane-bound flAPP was detected migrating as the standard doublet band of immature and mature forms of the protein between 90-100kDa in the TBSX fractions of the cortex and hippocampus (Figures 2C and 3B) (Burgess et al., 2008; Bush et al., 1990; Di Luca et al., 1998; Potempska et al., 1991; Van Nostrand et al.,

1991; Wahrle et al., 2008; Weidemann et al., 1989). This data was confirmed using antibodies specific for the C-terminus of APP, which detected the doublet bands in the TBSX-fractions but no bands in the TBS-fractions (data not shown). Thus, in the presence of increasing amount of Aβ42, small-volume tissue homogenizations for extraction of TBS-soluble proteins was consistent between samples, and proteins extracted by TBS and TBSX were specific for these fractions.

3.2 APP

An N-terminal antibody that detects both sAPP and flAPP was used to analyze APP in TBS, TBSX and GuHCl fractions of each brain region of 5xFAD and WT mice at 2 and 6 months (representative Western blots in Figures 2C and 3A-B). Results indicate that sAPP increased and flAPP decreased in the cortex and hippocampus from 2 to 6 months, compared to WT (Figure 3C-D). These results likely reflect the increased activity of BACE1 in these mice (Zhao et al., 2007). Surprisingly, although sAPP decreased in the disease-resistant cerebellum from 2 to 6 months, flAPP remained unchanged.

3.3 Aβ42

Aβ42 levels in the TBS, TBSX and GuHCl fractions of each brain region of 5xFAD mice at 2 and 6 months were measured via ELISA. Results indicate that Aβ42 increased significantly from 2 to 6 months in the cortex and hippocampus of 5xFAD mice in all extraction fractions (Figure 4A-C). In terms of the fold-increase from 2 to 6 months, the increase was greatest in the cortex, with a ~13-fold increase in the TBS and ~100-fold in GuHCl extractions (Figure 4D). In the hippocampus, Aβ42 levels showed similar significant increases in both TBS and GuHCl, with ~10- and ~70-fold increases, respectively. The levels of Aβ42 in the TBSX extractions of both the cortex and hippocampus increased by ~5-fold each, and Aβ42 in the cerebellum trended towards an increase, but this increase was not significant.

3.4 Murine apoE

The levels of m-apoE extracted by TBS, TBSX and GuHCl in the cortex and cerebellum of WT and 5xFAD mice were analyzed via ELISA. In WT mice, m-apoE was primarily localized to the TBSX fractions, with minimal m-apoE detected in TBS or GuHCl fractions (Figure 5A). However, the levels of m-apoE in 5xFAD mice were significantly greater in the TBS and GuHCl fractions compared to the TBSX fraction (Figure 5B). Further, in the 5xFAD mouse cortex, TBS-soluble m-apoE increased significantly from 2 to 6 months and GuHCl-soluble m-apoE was significantly elevated at 6 months.

In terms of the regional effects, m-apoE levels in the TBSX fractions of WT mice appeared greater in the cerebellum compared to the cortex. This is consistent with previously reported brain region-specific levels of apoE (Sullivan et al., 2004). However, m-apoE in the 5xFAD mice was consistently higher in the cortex than the cerebellum, likely reflecting the disease-susceptibility of the cortex and disease-resistance of the cerebellum.

3.5 Formic Acid extraction for Aβ42 and m-apoE

Although numerous protocols for serially extracting proteins from Aβ-Tg mice with diffuse and compact amyloid have utilized GuHCl as the terminal extraction buffer, the compact nature of mature amyloid plaques in human AD brain often requires the use of FA rather than, or in addition to, GuHCl (Delacourte et al., 2002; Hashimoto et al., 2002; Morishima-Kawashima et al., 2000; Patton et al., 2006; Wisniewski et al., 1995). Because 5xFAD mice develop significant amyloid plaque deposition at much earlier ages than previous Aβ-Tg mouse models, the possibility of GuHCl-insoluble dense-core amyloid was a concern. To

address this, Aβ42 and m-apoE in the cortex and cerebellum of 9-month-old 5xFAD mice were extracted in parallel with either GuHCl or FA (Figure 6A). FA extracted significantly more Aβ42 from the cortex than GuHCl (Figure 6B). As observed for 2- and 6-month-old mice, Aβ42 levels remained low in the cerebellum regardless of extraction buffer. In addition, significantly more m-apoE was extracted with FA in both the cortex and cerebellum of 9-month-old mice (Figure 6C).

4. Discussion

BACE1 cleaves flAPP, generating both Aβ42 and the resulting sAPP fragment. In 5xFAD mice BACE1 levels are increased over WT mice at 6 months. sAPP levels increased and flAPP decreased in the cortex and hippocampus at 2 months, and further at 6 months (Figure 3). These changes are logical, and likely reflect the age-dependent increase in BACE1 in 5xFAD mice (Zhao et al., 2007). Interestingly, the current experiments indicate that sAPP in 5xFAD mice increased compared to WT in the cortex and hippocampus at 2 months, when BACE1 levels should be “normal”. In contrast, in the cerebellum sAPP decreased from 2 to 6 months, yet flAPP remained unchanged. These results were inconsistent, assuming that total APP levels remain constant. Further, although Aβ42 in the cerebellum remained low, the levels trend towards an increase by 6 months. These results are also inconsistent with the decrease in sAPP. Although further study is needed, these results may suggest potential cerebellum-dependent processing of APP by proteases other than BACE1, or perhaps increased degradation of BACE1-generated sAPP fragments.

Recent research has focused on soluble assemblies of Aβ as the proximal cause of synaptic and neuronal loss and the eventual dementia associated with AD (Counts et al., 2006; Klein et al., 2001; Love et al., 2006; Thal et al., 2006; Tomiyama et al., 2010; Yu et al., 2010a), and research from our lab has shown that soluble oligomeric Aβ42 is the most toxic species *in vitro* (Dahlgren et al., 2002; Manelli et al., 2007). The transgenic 5xFAD mouse line was developed to maximize the production of Aβ42, and these mice contain soluble oligomeric Aβ42 *in vivo*, as measured by dot-blot analysis, that may be responsible for hippocampal-dependent memory loss at 6 months (Oakley et al., 2006; Ohno et al., 2006). Unfortunately, previous behavioral tests on these mice were conducted at 5-6 months when plaques were already abundant, making it difficult to attribute cognitive or behavioral deficits to a specific aspect of Aβ pathology. The present study indicates that soluble Aβ42 is detectable at 2 months, primarily in the cortex and hippocampus, possibly representing soluble oligomers that form prior to the deposition of amyloid. Although the majority of Aβ42 (~97-99%) extracted into the GuHCl fractions of the cortex and hippocampus at both 2 and 6 months, the fold-increase in TBS-soluble Aβ42 provides evidence for the development of a soluble species of the peptide. Importantly, the greatest increases in total Aβ42 in 5xFAD mice were in disease-susceptible brain regions, mimicking Aβ pathology in humans with AD. Specifically, Aβ42 increased significantly in the cortex and hippocampus (Thal et al., 2008). In addition, Aβ42 required FA for maximal extraction of insoluble protein, suggesting the presence of dense-core plaques by 9 months similar to those detected in AD brain. Although insoluble Aβ42 likely represents extracellular amyloid, a portion may be Aβ42 deposited intraneuronally (Oakley et al., 2006), possibly reflecting increased uptake of soluble Aβ42 species generated in younger mice and its subsequent conversion to insoluble peptide deposits as mice age. The appearance of toxic oligomeric Aβ42 in 6-month-old 5xFAD mice underscores the importance of biochemically analyzing well-defined brain regions of both young and old mice, in order to locate the region(s) responsible for producing the true toxic Aβ42 species. Although Aβ42 increased in the cortex and hippocampus, levels in the disease-susceptible cerebellum did not increase significantly. Thus, one possible explanation for the regional specificity of Aβ42 toxicity is that it is cell type-specific, affecting neurons

in the cortex and hippocampus but not the cerebellum, or is due to alternative conformational species of the peptide that are absent from the cerebellum.

The current method optimally extracts m-apoE from WT mice, such that it is primarily extracted into the TBSX fraction (Figure 5) due to apoE's association with lipoprotein particles and in vesicles. Human apoE (h-apoE) also extracts primarily into these TBSX fractions in mice expressing human apoE under the control of the mouse apoE promotor and regulatory elements ((Youmans, 2010), unpublished data and (Sullivan et al., 1997)). However, in 5xFAD mice, in the presence of significant levels of Aβ42, apoE was no longer detected in the TBSX fraction but was present in the TBS and GuHCl fractions. Thus, the extraction profile for m-apoE changes in the presence of Aβ42. This extraction profile of m-apoE parallels that for Aβ42. ApoE is an established component of amyloid plaques in AD brain, and increased m-apoE in GuHCl fractions with age confirming a role of m-apoE in amyloid deposition in 5xFAD brain as well. This data is supported by previous work in which 17-month Aβ-Tg mice showed increased insoluble m-apoE in the GuHCl fractions (Naidu et al., 2001), and indicates a potentially altered trafficking or storage pattern for m-apoE in the presence of elevated Aβ42 levels, although the mechanism(s) responsible for this change require further analysis. Similar findings have been reported for α-synuclein, another brain protein thought to cause toxicity due to abnormal aggregation properties, where researchers observed a decrease in membrane-apoE of human astrocytes following α-synuclein treatment (Koob et al., 2010). In addition, m-apoE levels appeared greatest in the cerebellum of WT mice at both 2 and 6 months, as expected (Sullivan et al., 2004). However, in 5xFAD mice m-apoE levels were greatest in the cortex at both ages. These results suggest that, in addition to shifting the solubility of apoE, Aβ42 may also shift its region-specific expression within the brain. Thus, the protein extraction protocol described appears to be a useful tool for identifying the extraction profiles of m-apoE in the presence or absence of Aβ42, and also the effects of Aβ42 on the region-specific expression of apoE.

Research Highlights

- Established sequential protein extraction method for low and high brain amyloid
- Measured age- and brain region-specific solubility of Aβ42 and m-apoE in 5xFAD mice
- Aβ42 and m-apoE are primarily TBS- or GuHCl- rather than TBSX-soluble
- Aβ42 and m-apoE require formic acid rather than GuHCl for efficient extraction

Acknowledgments

Current funding for the LaDu lab includes NIH (NIA) P01AG03012801, Alzheimer's Association ZEN-08-99900, UIC CCTS Pilot grant UL1RR029879, and an anonymous foundation grant.

6. References

Aoki M, Volkmann I, Tjernberg LO, Winblad B, Bogdanovic N. Amyloid beta-peptide levels in laser capture microdissected cornu ammonis 1 pyramidal neurons of Alzheimer's brain. Neuroreport 2008;19:1085–9. [PubMed: 18596605]

Bales KR, Liu F, Wu S, Lin S, Koger D, DeLong C, Hansen JC, Sullivan PM, Paul SM. Human APOE isoform-dependent effects on brain beta-amyloid levels in PDAPP transgenic mice. The Journal of neuroscience 2009;29:6771–9. [PubMed: 19474305]

Belinson H, Lev D, Masliah E, Michaelson DM. Activation of the amyloid cascade in apolipoprotein E4 transgenic mice induces lysosomal activation and neurodegeneration resulting in marked cognitive deficits. J Neurosci 2008;28:4690–701. [PubMed: 18448646]

Brecht WJ, Harris FM, Chang S, Tesseur I, Yu GQ, Xu Q, Dee Fish J, Wyss-Coray T, Buttini M, Mucke L, Mahley RW, Huang Y. Neuron-specific apolipoprotein e4 proteolysis is associated with increased tau phosphorylation in brains of transgenic mice. J Neurosci 2004;24:2527–34. [PubMed: 15014128]

Burgess BL, Parkinson PF, Racke MM, Hirsch-Reinshagen V, Fan J, Wong C, Stukas S, Theroux L, Chan JY, Donkin J, Wilkinson A, Balik D, Christie B, Poirier J, Lutjohann D, Demattos RB, Wellington CL. ABCG1 influences brain cholesterol synthesis but does not affect amyloid precursor protein or apolipoprotein E metabolism in vivo. J Lipid Res 2008;49:1254–67. [PubMed: 18314463]

Bush AI, Martins RN, Rumble B, Moir R, Fuller S, Milward E, Currie J, Ames D, Weidemann A, Fischer P, et al. The amyloid precursor protein of Alzheimer's disease is released by human platelets. The Journal of biological chemistry 1990;265:15977–83. [PubMed: 2118534]

Caselli RJ, Walker D, Sue L, Sabbagh M, Beach T. Amyloid load in nondemented brains correlates with APOE e4. Neurosci Lett 2010;473:168–71. [PubMed: 20153809]

Cataldo AM, Petanceska S, Terio NB, Peterhoff CM, Durham R, Mercken M, Mehta PD, Buxbaum J, Haroutunian V, Nixon RA. Abeta localization in abnormal endosomes: association with earliest Abeta elevations in AD and Down syndrome. Neurobiol Aging 2004;25:1263–72. [PubMed: 15465622]

Christensen DZ, Schneider-Axmann T, Lucassen PJ, Bayer TA, Wirths O. Accumulation of intraneuronal Abeta correlates with ApoE4 genotype. Acta Neuropathol 2010;119:555–66. [PubMed: 20217101]

Cizas P, Budvytyte R, Morkuniene R, Moldovan R, Broccio M, Losche M, Niaura G, Valincius G, Borutaite V. Size-dependent neurotoxicity of beta-amyloid oligomers. Archives of biochemistry and biophysics 2010;496:84–92. [PubMed: 20153288]

Counts SE, Nadeem M, Lad SP, Wuu J, Mufson EJ. Differential expression of synaptic proteins in the frontal and temporal cortex of elderly subjects with mild cognitive impairment. J Neuropathol Exp Neurol 2006;65:592–601. [PubMed: 16783169]

Dahlgren KN, Manelli AM, Stine WB Jr. Baker LK, Krafft GA, LaDu MJ. Oligomeric and fibrillar species of amyloid-beta peptides differentially affect neuronal viability. J Biol Chem 2002;277:32046–53. [PubMed: 12058030]

David HA, Gunnink JL. The Paired t Test Under Artificial Pairing. The American Statistician 1997;51:9–12.

Delacourte A, Sergeant N, Champain D, Wattez A, Maurage CA, Lebert F, Pasquier F, David JP. Nonoverlapping but synergetic tau and APP pathologies in sporadic Alzheimer's disease. Neurology 2002;59:398–407. [PubMed: 12177374]

Di Luca M, Pastorino L, Bianchetti A, Perez J, Vignolo LA, Lenzi GL, Trabucchi M, Cattabeni F, Padovani A. Differential level of platelet amyloid beta precursor protein isoforms: an early marker for Alzheimer disease. Archives of neurology 1998;55:1195–200. [PubMed: 9740113]

Durakoglugil MS, Chen Y, White CL, Kavalali ET, Herz J. Reelin signaling antagonizes beta-amyloid at the synapse. Proceedings of the National Academy of Sciences of the United States of America 2009;106:15938–43. [PubMed: 19805234]

Elliott DA, Tsoi K, Holinkova S, Chan SL, Kim WS, Halliday GM, Rye KA, Garner B. Isoform-specific proteolysis of apolipoprotein-E in the brain. Neurobiology of aging 2009;32:257–71. [PubMed: 19278755]

Gouras GK, Tampellini D, Takahashi RH, Capetillo-Zarate E. Intraneuronal beta-amyloid accumulation and synapse pathology in Alzheimer's disease. Acta neuropathologica 2010;119:523–41. [PubMed: 20354705]

Han S-H, Hulette C, Saunders AM, Einstein G, Pericak-Vance M, Strittmatter WJ, Roses AD, Schmechel DE. Apolipoprotein E is present in hippocampal neurons without neurofibrillary tangles in Alzheimer's disease and in age-matched controls. Exp. Neurol 1994;128:13–26. [PubMed: 8070517]

Hashimoto T, Wakabayashi T, Watanabe A, Kowa H, Hosoda R, Nakamura A, Kanazawa I, Arai T, Takio K, Mann DM, Iwatsubo T. CLAC: a novel Alzheimer amyloid plaque component derived

from a transmembrane precursor, CLAC-P/collagen type XXV. The EMBO journal 2002;21:1524–34. [PubMed: 11927537]

Hirsch-Reinshagen V, Maia LF, Burgess BL, Blain JF, Naus KE, McIsaac SA, Parkinson PF, Chan JY, Tansley GH, Hayden MR, Poirier J, Van Nostrand W, Wellington CL. The absence of ABCA1 decreases soluble apoE levels but does not diminish amyloid deposition in two murine models of Alzheimer's disease. J Biol Chem 2005;280:43243–56. [PubMed: 16207707]

Kawarabayashi T, Shoji M, Younkin LH, Wen-Lang L, Dickson DW, Murakami T, Matsubara E, Abe K, Ashe KH, Younkin SG. Dimeric amyloid beta protein rapidly accumulates in lipid rafts followed by apolipoprotein E and phosphorylated tau accumulation in the Tg2576 mouse model of Alzheimer's disease. J Neurosci 2004;24:3801–9. [PubMed: 15084661]

Kawarabayashi T, Younkin LH, Saido TC, Shoji M, Ashe KH, Younkin SG. Age-dependent changes in brain, CSF, and plasma amyloid (beta) protein in the Tg2576 transgenic mouse model of Alzheimer's disease. J Neurosci 2001;21:372–81. [PubMed: 11160418]

Kim J, Basak JM, Holtzman DM. The role of apolipoprotein E in Alzheimer's disease. Neuron 2009;63:287–303. [PubMed: 19679070]

Klein WL, Krafft GA, Finch CE. Targeting small Abeta oligomers: the solution to an Alzheimer's disease conundrum? Trends Neurosci 2001;24:219–24. [PubMed: 11250006]

Koob AO, Paulino AD, Masliah E. GFAP reactivity, apolipoprotein E redistribution and cholesterol reduction in human astrocytes treated with alpha-synuclein. Neuroscience letters 2010;469:11–4. [PubMed: 19932737]

Krul, E.; Cole, T. Quantitation of apolipoprotein E. Methods in Enzymology. Academic Press; New York: 1996. p. 170-87.

Lesne S, Koh MT, Kotilinek L, Kayed R, Glabe CG, Yang A, Gallagher M, Ashe KH. A specific amyloid-beta protein assembly in the brain impairs memory. Nature 2006;440:352–7. [PubMed: 16541076]

Lippel K, Tyroler HA, Gotto A Jr. Brewer HB, Albers JJ, Scanu A, Alaupovic P. Workshop on apolipoprotein quantification. Arteriosclerosis 1983;3:452–64. [PubMed: 6626035]

Liu Q, Zerbinatti CV, Zhang J, Hoe HS, Wang B, Cole SL, Herz J, Muglia L, Bu G. Amyloid precursor protein regulates brain apolipoprotein E and cholesterol metabolism through lipoprotein receptor LRP1. Neuron 2007;56:66–78. [PubMed: 17920016]

Love S, Siew LK, Dawbarn D, Wilcock GK, Ben-Shlomo Y, Allen SJ. Premorbid effects of APOE on synaptic proteins in human temporal neocortex. Neurobiol Aging 2006;27:797–803. [PubMed: 15979210]

Manelli AM, Bulfinch LC, Sullivan PM, LaDu MJ. Abeta42 neurotoxicity in primary co-cultures: effect of apoE isoform and Abeta conformation. Neurobiol Aging 2007;28:1139–47. [PubMed: 16837105]

Mastrangelo MA, Bowers WJ. Detailed immunohistochemical characterization of temporal and spatial progression of Alzheimer's disease-related pathologies in male triple-transgenic mice. BMC neuroscience 2008;9:81. [PubMed: 18700006]

Morishima-Kawashima M, Oshima N, Ogata H, Yamaguchi H, Yoshimura M, Sugihara S, Ihara Y. Effect of apolipoprotein E allele epsilon4 on the initial phase of amyloid beta-protein accumulation in the human brain. The American journal of pathology 2000;157:2093–9. [PubMed: 11106581]

Naidu A, Catalano R, Bales K, Wu S, Paul SM, Cordell B. Conversion of brain apolipoprotein E to an insoluble form in a mouse model of Alzheimer disease. Neuroreport 2001;12:1265–70. [PubMed: 11338204]

Oakley H, Cole SL, Logan S, Maus E, Shao P, Craft J, Guillozet-Bongaarts A, Ohno M, Disterhoft J, Van Eldik L, Berry R, Vassar R. Intraneuronal beta-amyloid aggregates, neurodegeneration, and neuron loss in transgenic mice with five familial Alzheimer's disease mutations: potential factors in amyloid plaque formation. J Neurosci 2006;26:10129–40. [PubMed: 17021169]

Oddo S, Caccamo A, Shepherd JD, Murphy MP, Golde TE, Kayed R, Metherate R, Mattson MP, Akbari Y, LaFerla FM. Triple-transgenic model of Alzheimer's disease with plaques and tangles: intracellular Abeta and synaptic dysfunction. Neuron 2003;39:409–21. [PubMed: 12895417]

Ohno M, Chang L, Tseng W, Oakley H, Citron M, Klein WL, Vassar R, Disterhoft JF. Temporal memory deficits in Alzheimer's mouse models: rescue by genetic deletion of BACE1. Eur J Neurosci 2006;23:251–60. [PubMed: 16420434]

Patton RL, Kalback WM, Esh CL, Kokjohn TA, Van Vickle GD, Luehrs DC, Kuo YM, Lopez J, Brune D, Ferrer I, Masliah E, Newel AJ, Beach TG, Castano EM, Roher AE. Amyloid-beta peptide remnants in AN-1792-immunized Alzheimer's disease patients: a biochemical analysis. The American journal of pathology 2006;169:1048–63. [PubMed: 16936277]

Potempska A, Styles J, Mehta P, Kim KS, Miller DL. Purification and tissue level of the beta-amyloid peptide precursor of rat brain. The Journal of biological chemistry 1991;266:8464–9. [PubMed: 1673681]

Querfurth HW, LaFerla FM. Alzheimer's disease. The New England journal of medicine 2010;362:329–44. [PubMed: 20107219]

Schmitz C, Rutten BP, Pielen A, Schafer S, Wirths O, Tremp G, Czech C, Blanchard V, Multhaup G, Rezaie P, Korr H, Steinbusch HW, Pradier L, Bayer TA. Hippocampal neuron loss exceeds amyloid plaque load in a transgenic mouse model of Alzheimer's disease. Am J Pathol 2004;164:1495–502. [PubMed: 15039236]

Sullivan PM, Han B, Liu F, Mace BE, Ervin JF, Wu S, Koger D, Paul S, Bales KR. Reduced levels of human apoE4 protein in an animal model of cognitive impairment. Neurobiology of aging. 2009

Sullivan PM, Mace BE, Maeda N, Schmechel DE. Marked regional differences of brain human apolipoprotein E expression in targeted replacement mice. Neuroscience 2004;124:725–33. [PubMed: 15026113]

Sullivan PM, Mezdour H, Aratani Y, Knouff C, Najib J, Reddick RL, Quarfordt SH, Maeda N. Targeted replacement of the mouse apolipoprotein E gene with the common human APOE3 allele enhances diet-induced hypercholesterolemia and atherosclerosis. J Biol Chem 1997;272:17972–80. [PubMed: 9218423]

Thal DR, Capetillo-Zarate E, Del Tredici K, Braak H. The development of amyloid beta protein deposits in the aged brain. Science of aging knowledge environment 2006;2006:re1. [PubMed: 16525193]

Thal DR, Griffin WS, Braak H. Parenchymal and vascular Abeta-deposition and its effects on the degeneration of neurons and cognition in Alzheimer's disease. Journal of cellular and molecular medicine 2008;12:1848–62. [PubMed: 18624777]

Tomiyama T, Matsuyama S, Iso H, Umeda T, Takuma H, Ohnishi K, Ishibashi K, Teraoka R, Sakama N, Yamashita T, Nishitsuji K, Ito K, Shimada H, Lambert MP, Klein WL, Mori H. A mouse model of amyloid beta oligomers: their contribution to synaptic alteration, abnormal tau phosphorylation, glial activation, and neuronal loss in vivo. The Journal of neuroscience 2010;30:4845–56. [PubMed: 20371804]

Van Nostrand WE, Farrow JS, Wagner SL, Bhasin R, Goldgaber D, Cotman CW, Cunningham DD. The predominant form of the amyloid beta-protein precursor in human brain is protease nexin 2. Proceedings of the National Academy of Sciences of the United States of America 1991;88:10302–6. [PubMed: 1946448]

Wahrle SE, Jiang H, Parsadanian M, Kim J, Li A, Knoten A, Jain S, Hirsch-Reinshagen V, Wellington CL, Bales KR, Paul SM, Holtzman DM. Overexpression of ABCA1 reduces amyloid deposition in the PDAPP mouse model of Alzheimer disease. J Clin Invest 2008;118:671–82. [PubMed: 18202749]

Wahrle SE, Shah AR, Fagan AM, Smemo S, Kauwe JS, Grupe A, Hinrichs A, Mayo K, Jiang H, Thal LJ, Goate AM, Holtzman DM. Apolipoprotein E levels in cerebrospinal fluid and the effects of ABCA1 polymorphisms. Mol Neurodegener 2007;2:7. [PubMed: 17430597]

Weidemann A, Konig G, Bunke D, Fischer P, Salbaum JM, Masters CL, Beyreuther K. Identification, biogenesis, and localization of precursors of Alzheimer's disease A4 amyloid protein. Cell 1989;57:115–26. [PubMed: 2649245]

Wisniewski T, Lalowski M, Golabek A, Vogel T, Frangione B. Is Alzheimer's disease an apolipoprotein E amyloidosis? Lancet 1995;345:956–8. [PubMed: 7715296]

Youmans, KL.; American Society for Neurochemistry. Transactions of the American Society for Neurochemistry. Santa Fe; NM: 2010. The Effects of Human apoE on Amyloid-beta (42) Pathology and Synaptic Loss in a Novel Transgenic Mouse Model.

Yu C, Nwabuisi-Heath E, Laxton K, Ladu MJ. Endocytic pathways mediating oligomeric Abeta42 neurotoxicity. Mol Neurodegener 2010a;5:19. [PubMed: 20478062]

Yu C, Youmans KL, Ladu MJ. Proposed mechanism for lipoprotein remodelling in the brain. Biochim Biophys Acta 2010b;1801:819–23. [PubMed: 20470897]

Zerbinatti CV, Wahrle SE, Kim H, Cam JA, Bales K, Paul SM, Holtzman DM, Bu G. Apolipoprotein E and low density lipoprotein receptor-related protein facilitate intraneuronal Abeta42 accumulation in amyloid model mice. The Journal of biological chemistry 2006;281:36180–6. [PubMed: 17012232]

Zhao J, Fu Y, Yasvoina M, Shao P, Hitt B, O'Connor T, Logan S, Maus E, Citron M, Berry R, Binder L, Vassar R. Beta-site amyloid precursor protein cleaving enzyme 1 levels become elevated in neurons around amyloid plaques: implications for Alzheimer's disease pathogenesis. J Neurosci 2007;27:3639–49. [PubMed: 17409228]

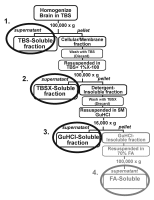

Figure 1.
Simplified overview of sequential extraction protocol.

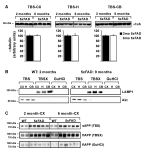

Figure 2. Serial extraction is reproducible and consistent

Representative WB of α-tubulin in 25μg of TBS-extracted cortex (CX), hippocampus (H) and cerebellum (CB), from 2- and 6-month 5xFAD mice (A, Top). Quantification of α-tubulin band intensity was performed using ImageJ, with mean α-tubulin values set to 100 and plotted below, as the mean ± SEM (A, Bottom). Representative WB of LAMP1 and Akt in equal extraction volumes of TBS-, TBSX- and GuHCl-extracted CX, H and CB from 2-month WT and 9-month 5xFAD mice are analyzed as markers of correct fractionation in the presence of significant Aβ42 (B). Representative WB of soluble APP (sAPP) and full-length APP (flAPP) in equal extraction volumes of TBS-, TBSX- and GuHCl-extracted CX from 2- and 6-month WT and 5xFAD mice (C).

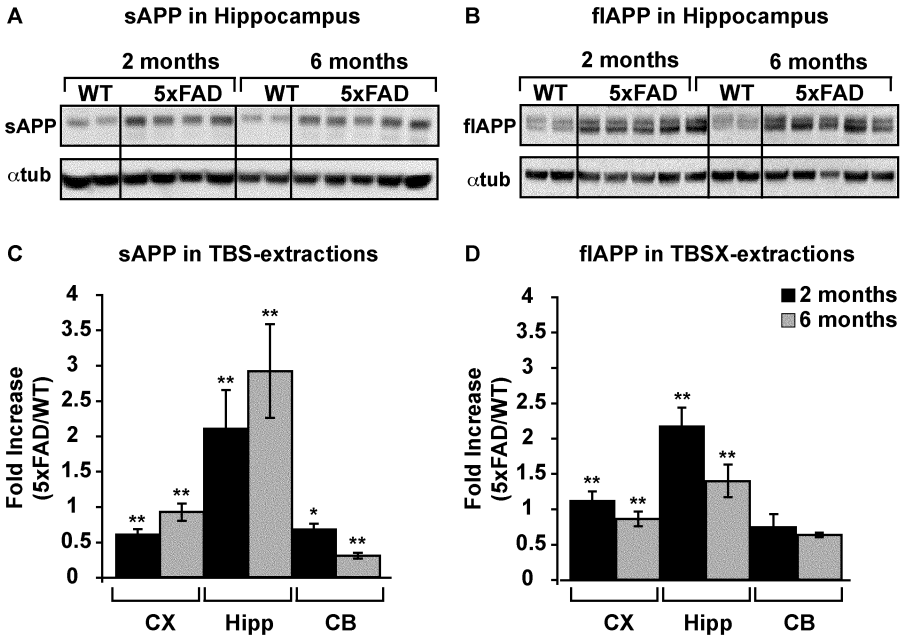

Figure 3. APP increases in TBS- and TBSX-extractions in 5xFAD mice

Representative WB of APP and αtubulin in 25μg TBS- (A) and TBSX-extracted (B) hippocampus of 2- and 6-month WT and 5xFAD mice. Quantification of APP/αtubulin was performed using ImageJ, and the fold-increase in 5xFAD mice vs WT at either 2 or 6 months is plotted (C-D). Data are presented as the mean ± SEM, * $p < 0.05$, ** $p < 0.01$.

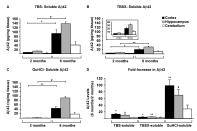

Figure 4. Aβ42 increases in the cortex and hippocampus with age

Aβ42 in CX, H and CB of 2- and 6-month 5xFAD mice was measured by ELISA. Samples were diluted to bring Aβ42 into the working range of the assay, and levels are given as pg/mg tissue for TBS- (A) and TBSX- (B) extractions, and as ng/mg for GuHCl-extractions (C). The fold-increase in Aβ42 from 2 to 6 months for each brain region and extraction is plotted (D). n= 5 mice at each age. Data are presented as the mean ± SEM, * $p < 0.05$, ** $p < 0.01$, # $p < 0.001$.

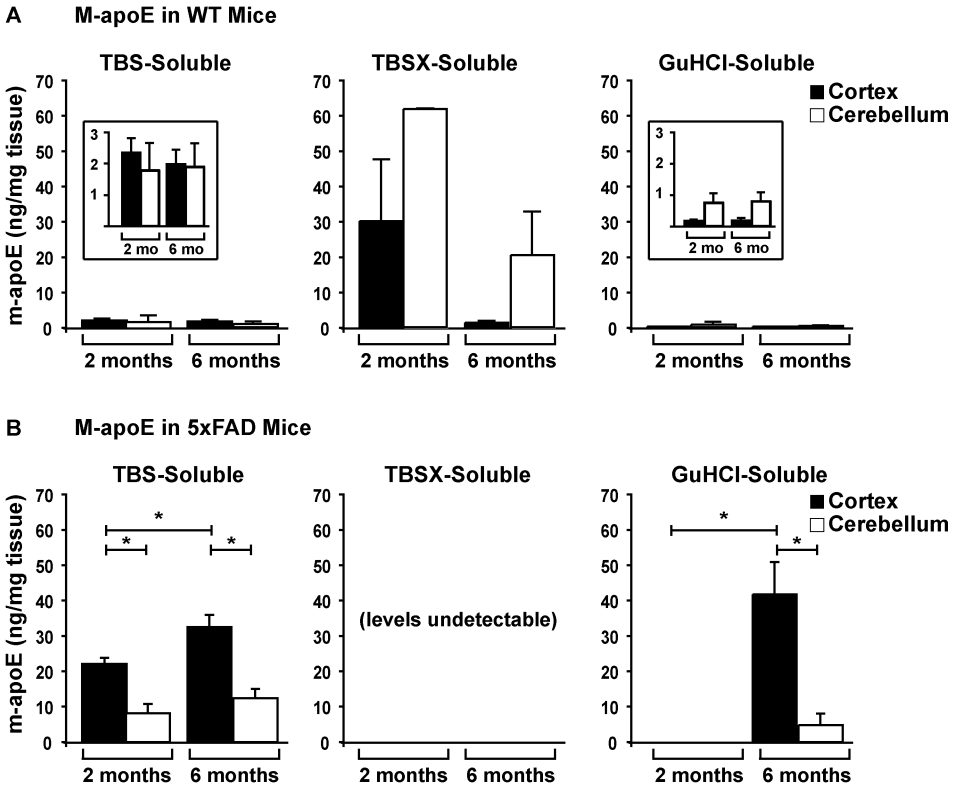

Figure 5. Murine apoE moves into the TBS- and GuHCl-soluble fractions in the presence of Aβ

M-apoE in CX and CB of 2- and 6-month WT (A) and 5xFAD (B) mice was measured by ELISA. Samples were diluted to bring m-apoE into the working range of the assay, and levels are given as ng/mg tissue for TBS-, TBSX- and GuHCl-extractions. n= 4-5 mice at each age. Data are presented as the mean ± SEM, * $p < 0.05$.

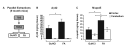

Figure 6. Formic acid extracts additional Aβ42 and m-apoE compared to GuHCl in old 5xFAD mice

The CX and CB of 9-month 5xFAD mice were extracted in parallel with 5M GuHCl or 70% FA as outlined briefly (A). Levels of Aβ42 (B) and m-apoE (C) were measured in each extraction by ELISA, as described previously. n= 5 mice at each age. Data are presented as the mean ± SEM, * $p < 0.05$, # $p < 0.001$.